Cancer Immunology, Immunotherapy (2018) 67:761–774
https://doi.org/10.1007/s00262-018-2130-3

ORIGINAL ARTICLE

TriCurin, a synergistic formulation of curcumin, resveratrol, and epicatechin gallate, repolarizes tumor-associated macrophages and triggers an immune response to cause suppression of HPV+ tumors

Sumit Mukherjee[1,2,3] · Rahman Hussaini[3] · Richard White[3] · Doaa Atwi[3] · Angela Fried[1,3] · Samay Sampat[4] · Longzhu Piao[5,6] · Quintin Pan[5,6] · Probal Banerjee[2,3]

Received: 29 June 2017 / Accepted: 10 February 2018 / Published online: 16 February 2018

Abstract

Our earlier studies reported a unique potentiated combination (TriCurin) of curcumin (C) with two other polyphenols. The TriCurin-associated C displays an IC50 in the low micromolar range for cultured HPV+ TC-1 cells. In contrast, because of rapid degradation in vivo, the TriCurin-associated C reaches only low nano-molar concentrations in the plasma, which are sub-lethal to tumor cells. Yet, injected TriCurin causes a dramatic suppression of tumors in TC-1 cell-implanted mice (TC-1 mice) and xenografts of Head and Neck Squamous Cell Carcinoma (HNSCC) cells in *nude/nude* mice. Here, we use the TC-1 mice to test our hypothesis that a major part of the anti-tumor activity of TriCurin is evoked by innate and adaptive immune responses. TriCurin injection repolarized arginase1^{high} (ARG1^{high}), IL10^{high}, inducible nitric oxide synthase^{low} (iNOS^{low}), IL12^{low} M2-type tumor-associated macrophages (TAM) into ARG1^{low}, IL10^{low}, iNOS^{high}, and IL12^{high} M1-type TAM in HPV+ tumors. The M1 TAM displayed sharply suppressed STAT3 and induced STAT1 and NF-kB(p65). STAT1 and NF-kB(p65) function synergistically to induce *iNOS* and *IL12* transcription. Neutralizing IL12 signaling with an IL12 antibody abrogated TriCurin-induced intra-tumor entry of activated natural killer (NK) cells and Cytotoxic T lymphocytes (CTL), thereby confirming that IL12 triggers recruitment of NK cells and CTL. These activated NK cells and CTL join the M1 TAM to elicit apoptosis of the E6+ tumor cells. Corroboratively, neutralizing IL12 signaling partially reversed this TriCurin-mediated apoptosis. Thus, injected TriCurin elicits an M2→M1 switch in TAM, accompanied by IL12-dependent intra-tumor recruitment of NK cells and CTL and elimination of cancer cells.

Keywords Curcumin · TriCurin · Papillomavirus · Tumor-associated macrophages · NK cells · CTL

Abbreviations

ARG1	Arginase-1
C	Curcumin
CD8	Cluster of differentiation 8 protein
CD8α	Cluster of differentiation 8 alpha

Rahman Hussaini and Richard White contributed equally.

Electronic supplementary material The online version of this article (https://doi.org/10.1007/s00262-018-2130-3) contains supplementary material, which is available to authorized users.

✉ Probal Banerjee
probal.banerjee@csi.cuny.edu

[1] CUNY Doctoral Program in Biochemistry, CUNY Graduate Center, New York, NY 10016, USA

[2] Department of Chemistry, Building 6S, The City University of New York at The College of Staten Island, 2800 Victory Boulevard, Staten Island, NY 10314, USA

[3] The Center for Developmental Neuroscience, City University of New York at The College of Staten Island, 2800 Victory Boulevard, Staten Island, NY 10314, USA

[4] College of Arts and Science, New York University, New York, NY 10003, USA

[5] Department of Otolaryngology-Head and Neck Surgery, The Ohio State University Medical Center, Columbus, OH 43210, USA

[6] Arthur G. James Cancer Hospital and Richard J. Solove Research Institute, The Ohio State University Comprehensive Cancer Center, Columbus, OH 43210, USA

CTL	Cytotoxic T lymphocytes
CUNY	City University of New York
E	Epicatechin gallate
E6 16/18	Early 6 protein 16/18
E7	Early 7 protein
HaRas	Harvey ras protein
HCl	Hydrochloric acid
HNSCC	Head and neck squamous cell carcinoma
HPV	Human papillomavirus
IACUC	Institutional Animal Care and Use Committee
Iba1	Ionized calcium-binding adapter molecule 1
IF	Integrated fluorescence
IFNγ	Interferon gamma
IgG	Immunoglobin G
IL10	Interleukin-10
IL12	Interleukin-12
iNOS	Inducible nitric oxide synthase
LEEP	Loop electrosurgical excision procedure
LR	Lower right
NCr	Athymic nude mice
NKp46	Natural killer cell p-46-related protein
NOS2	Nitric oxide synthase 2
PFA	Paraformaldehyde
P-NF-kB	Phospho-NF-kB
P-p65	Phospho-p65
P-ser	Phosphor-serine
P-STAT1/3	Phospho-STAT1/3
P-Tyr	Phospho-tyrosine
R	Resveratrol
S.E.	Standard error
SEM	Standard error of the mean
SSC	Saline-sodium citrate
TAM	Tumor-associated macrophage
TriCur + IL12Ab	'IL12 antibody infusion followed by TriCurin treatment' group
UL	Upper left
UMSCC47	University of Michigan-squamous cell carcinoma-47
UR	Upper right
w/v	Weight/volume

Introduction

The human papillomavirus (HPV) is the major risk factor for cervical cancer that claims numerous lives globally and is a major threat to women especially in the developing countries where screening and vaccinations are not affordable or realistic due to the lack of infrastructure. The incidence of cervical cancer is rather low in the developed countries because of extensive screening programs [1–3]. Though the availability of two vaccines, Cervarix® and Gardasil®, offers preventive measures against the usual tumorigenic HPV16/18+ cervical lesions, effective therapy for post-infection lesions is currently unavailable [4]. High-risk HPV16+ infection has also emerged as an etiologic factor for the development of head and neck squamous cell carcinoma (HNSCC), with new cases escalating worldwide. The standard of care for HNSCC consists of surgery, radiation therapy, chemotherapy, or a combination of treatments, which have significant side effects and/or are associated with high morbidity [2, 5, 6]. This emphasizes the need for safe therapeutic approaches to treat HPV+ cervical cancer and HNSCC.

In earlier studies, we developed a formulation, termed TriCurin, containing curcumin (C) with two other food-derived natural polyphenols, resveratrol (R) and epicatechin gallate (E) at a unique and synergistic molar ratio. TriCurin is non-toxic to normal cells and selectively eliminates cancer cells in vitro and also in HaRas+, HPV16 E6+ and E7+ TC-1 cell-evoked mouse tumors and xenografts of HNSCC tumors in athymic *nude/nude* mice (NCr) [7, 8]. Poor bioavailability of C seriously limits its anti-tumor efficacy and the increased potency of TriCurin against cancer cells has been attributed to the stabilization of C in the presence of R and E and increased uptake of C from TriCurin into tumor cells [8]. Thus, such improved delivery of C has enabled us to use TriCurin to efficiently eliminate a wide array of tumor cells [7–15]. Although enhanced delivery increases the plasma concentration of C, it never reaches beyond the low nanomolar range, which is not high enough to cause direct elimination of cancer cells, which requires micromolar curcumin (Sumit Mukherjee et al., unpublished). We have postulated that the nano-molar level of C in the plasma is sufficient to activate the innate and adaptive immune system against tumor [12, 13, 16–21].

We demonstrate here for the first time that TriCurin treatment of tumor-bearing mice leads to an overall repolarization of the milieu of HPV+ tumor-associated macrophages from an M2 state to M1 phenotype. In addition, we also demonstrate that TriCurin-evoked repolarization of TAM is associated with intra-tumor recruitment of activated NK cells and CTL which are known to have tumoricidal activity [16, 17, 19, 20]. These changes in the tumor microenvironment play a major role in TriCurin-evoked elimination of HPV+ tumors [1, 7, 8, 12, 14].

Promising clinical trials using chimeric antigen receptor (CAR) T-cell treatment and regulators of T-cell activation (checkpoint inhibitors) have recently yielded immunotherapy drugs for cancer. Our therapeutic strategy using TriCurin also depends on the activation of the immune system against tumor, but unlike other approaches, it involves

a highly potent agent (TriCurin), which does not elicit the side effects commonly experienced in other therapies [22, 23]. Thus, TriCurin is a promising immunotherapeutic agent for various types of cancer.

Materials and methods

Animals

Please see the 'Animal Source' subsection under 'Compliance With Ethical Standards'.

Preparation of TriCurin

1.28 mM + TriCurin solution in PBS was prepared according to our earlier reports [7, 8].

Cell culture

HPV+ mouse TC-1 cells and UMSCC47 human cells were procured, authenticated, and cultured as reported earlier. HPV16+ UMSCC47 HNSCC cells were obtained from Dr. Thomas Carey (University of Michigan) [7, 8].

Implantation of cancer cells in mice

To generate the TC-1 mouse model, experiments were performed according to our previous report [8]. The tumors were allowed to grow to a diameter of 0.5 cm before intra-tumor infusion of TriCurin.

To generate the pre-clinical UMSCC47-derived HNSCC (UMSCC47) xenograft tumors in athymic *nude/nude* mice (NCr), experiments were performed according to our earlier report. The tumors were allowed to be palpable before intra-tumor infusion of TriCurin [7].

Treatment of pre-clinical HPV+ tumor-bearing mice with TriCurin

When the TC-1 tumors assumed the approximate length of 0.5 cm, eight mice were randomly divided into two groups: "Vehicle" (PBS plus 5% DMSO) ($n = 6$), "TriCurin" ($n = 6$), and "TriCurin + IL12Ab" ($n = 3$). Each tumor was marked into four quadrants and 2.5 µl of the 1.28 mM + TriCurin solution (or Vehicle) was infused into each of the four quadrants every 24 h for 5 days (final estimated intra-tumor concentration for each injection: 64 µM+). On the sixth day from the first treatment (the day of first treatment was marked as day 1) (TriCurin or Vehicle or TriCurin + IL12Ab), the mice were sacrificed, tumors extricated, and the final tumor volumes were measured by displacement of water. The Tumors were divided into two halves: one-half for preparing single-cell suspensions for post-immunostaining flow cytometry and the other half for immunohistochemistry and confocal microscopy.

Athymic mice (*nu/nu*) bearing human UMSCC47 cell-derived HNSCC xenograft tumors were treated with 1.28 mM + TriCurin (or Vehicle) and tumors were subsequently processed according to our earlier report [7].

Neutralization of IL12 signaling on NK cells and CTL by intra-peritoneal infusion of IL12Ab

On day 0 (24 h before the first TriCurin treatment) and day 3, each TC-1 implanted mouse in the TriCurin + IL12Ab group received intra-peritoneal injection of IL12-neutralizing Anti-IL12 (p40/p70) antibody (BD, 554,475) (60 µg, each dose) [24]. Mice in the other two groups (Vehicle and TriCurin) received rat serum (60 µg, per mouse, per dose) and subsequent drugs (Vehicle or TriCurin) as stated in the previous section.

Preparation of single-cell suspensions from TC-1 tumors and immunostaining for flow cytometry

One-half of the extricated TC-1 tumor was placed in RPMI-1640 medium containing 100 U/ml penicillin and 100 µg/ml streptomycin. Next, the tumors were rinsed with PBS and subsequently minced into 1–2-mm pieces and immersed in serum-free RPMI-1640 medium containing 0.05 mg/ml collagenase I (Fisher #NC0847850), 0.05 mg/ml collagenase IV (Fisher #ICN19511080), 0.025 mg/ml hyaluronidase IV (Fisher #NC9725814), 0.25 mg/ml DNase I, 100 U/ml penicillin, and 100 µg/ml streptomycin. The resultant cocktail was incubated at 37 °C for 15 min with periodic agitation in a mechanical shaker. The tumor digest was strained through a 70-µm nylon filter to remove undigested tissue fragments. The resultant single tumor cells were pelleted, washed with PBS, and fixed in 4% PFA [25].

For flow cytometry, 2 million fixed cells from each animal were immunostained as described earlier [12]. After each antibody treatment, the cells were pelleted and resuspended in wash buffers. Antibodies against Iba1 (C20) (1:50), iNOS (1:100), Arginase1 (1:100), NKp46 (1:100), active-caspase 3 (Asp175) (1:100), and E6 (1:75) were used for staining. Cells treated with the secondary antibody alone were used to set the threshold. The double-stained fluorescent events from ARG1+/Iba1+ and iNOS+/Iba1+ cells appeared as sub-populations in the upper right (UR) quadrant within the coordinates 520 nm (green for ARG1 or iNOS) (FL1-A) and 580 nm (red for Iba1) (FL2-A). Single-stained fluorescent events from the scatter plots and from Nkp46+ (580 nm, red) and E6+ (520 nm, green) cells appeared as sub-populations in the upper left (UL) and the lower right (LR) quadrants, respectively. Integrated fluorescence intensity was measured

for comparison between groups by multiplying the number of positive events (single-stained or double-stained cells) by the mean fluorescence intensity per event (cell).

Immunohistochemistry

Randomly chosen sections were subjected to pre-immunostaining antigen-retrieval using formamide: 2×SSC as reported earlier [7, 8, 12] only for IL12 and IL10 by treating with 0.1% (w/v) pepsin (Fisher, AC417071000) dissolved in 0.01 N HCl for 20 min at room temperature, followed by two PBS washes. For immunostaining, the sections were blocked overnight at 4 °C in 0.1% Triton X-100, 3% goat serum and 10% rabbit serum in 100 mM PBS, and then treated overnight with primary antibodies: anti-Iba1 (goat IgG) (C20) (sc28530) (1:50), iNOS (rabbit IgG) (NOS2 sc-651) (1:100), anti-Arginase1 (rabbit IgG) (sc-20150) (1:100), anti-STAT3 (rabbit IgG) (sc-7179) (1:100), anti-P-Tyr^{705}-STAT3 (goat IgG) (sc-7993) (1:100), anti-STAT1 (rabbit IgG) (sc-592) (1:100), anti-P-Tyr^{701}-STAT1 (mouse IgG) (sc-8394) (1:100), anti-p65 (NF-kB) (mouse IgG) (sc-8008), anti-P-Ser^{276}-p65 (NF-kB) (rabbit IgG) (sc-101749) (1:100), IL12p40 (rabbit IgG) (sc-7926) (1:100), IL10 (goat IgG) (sc-1783) (1:100), anti-NKp46 (rabbit IgG) (sc-292796) (1:100), anti-CD8-α (D-9) (mouse IgG) (sc-7970) (1:100), anti-E6 antibody (mouse IgG)(sc-460) (1:75) (Santa Cruz Biotechnology), and anti-active-caspase 3 (Asp175) (Rabbit IgG) (CST#9661, Cell Signaling Technology) (1:200). All antibodies were diluted in 2% goat serum plus 2% rabbit serum and 0.1% Triton X-100 in PBS (GRT-PBS). After washing three times with PBS, the respective secondary antibodies (Alexa Fluor 568 rabbit anti-goat, Alexa Fluor 488 goat anti-rabbit, Alexa Fluor 568 goat anti-rabbit, Alexa Fluor 633 rabbit anti-goat, Alexa Fluor 633 goat anti-mouse, Alexa Fluor 488 rabbit anti-goat, Alexa Fluor 568 goat anti-mouse, Alexa Fluor 633 goat anti-rabbit, and Alexa Fluor goat 488 anti-mouse) (Invitrogen) (1:1000 dilutions in GRT-PBS) were added to wells treated with the respective primary antibodies as well as those not treated with primary antibodies (2° Ab controls). Following overnight incubation at 4 °C and three washes with PBS, the sections were treated with HOECHST33342 (10 µg/ml) for 30 min at room temperature, followed by three washes with PBS and mounting on microscope slides with Gold anti-fade mounting fluid. Confocal Imaging was conducted using a Leica SP2 microscope from multiple randomly chosen fields.

ImageJ was used to quantify the fluorescence intensity for iNOS, ARG1, p65 (NF-kB), P-Ser^{276}-p65, STAT-1, P-Tyr^{701}-STAT1, NKp46, E6, anti-active-caspase 3 (Asp175), and HOECHST33342. The fluorescence intensity for each marker was normalized to HOECHST33342 intensity (blue). Since STAT3, STAT1, and p65 NF-kB displayed both induction as well as phosphorylation-mediated deactivation/activation, the HOECHST-normalized staining intensities were expressed both as P-STAT3/STAT3, P-STAT1/STAT1, and P-p65 NF-kB/p65 NF-kB, as well as P-STAT3/HOECHST, P-STAT1/HOECHST, and P-p65 NF-kB/HOECHST.

Statistical analysis

We used two-tailed *t* tests with unequal variance while comparing between two groups and one-way ANOVA with Tukey for post-hoc analysis to compare among three groups ($p \leq 0.05$ was considered as significant).

Results

Five days of TriCurin treatment is adequate to cause repolarization of tumor-associated macrophages from M2 to M1 phenotype in TC-1 tumor. Immunostaining of the tumors from the Vehicle and TriCurin groups revealed that the 'tumor-core' harbors mostly E6+ tumor cells, while the 'tumor-periphery' harbors mostly Iba1+ TAM (Supplementary Fig. 1) [8, 12]. TriCurin-evoked repolarization of ARG1^{high} M2 TAM into iNOS^{high} M1 TAM was studied using flow cytometry analysis of immunostained cells dissociated from Vehicle-treated and TriCurin-treated TC-1 tumors [8, 12]. The integrated fluorescence (IF) from ARG1+/Iba1+ (M2 TAM) (Fig. 1a, b) and iNOS/Iba1+(M1 TAM) (Fig. 1e, f) double-stained events occurring in the upper right (UR) quadrant (red ellipse) was used to quantitatively compare between the two groups. Whereas the Iba1+ cells in the tumor were ARG1^{high}/iNOS^{low} (Fig. 1a, e) in the Vehicle-treated mice, in the TriCurin-treated tumors, the Iba1+ cells were ARG1^{low}/iNOS^{high} (Fig. 1b, f). We observed a 55.5% decrease in ARG1 IF (Fig. 1c, d) and a 305% increase in iNOS IF (Fig. 1e, h). The intra-tumor iNOS ^{high} M1 TAM liberate NO, which is expected to be cytotoxic toward the surrounding tumor cells [12, 13, 26].

The Iba1 IF of these double-stained events (ARG1+ or iNOS+) was also sharply dissimilar between the two groups. TriCurin treatment elicited an 80% decrease in Iba1 IF in the ARG1+ cells in the tumor (relative to Vehicle-treated) (Fig. 1i), but the Iba1 IF in the iNOS+ cells in the TriCurin-treated tumors was 989% higher than in the Vehicle-treated tumors (Fig. 1j). In contrast, the total Iba1 IF (total number of Iba1+ cells in the iNOS+/Iba1+ and ARG1+/Iba1+ populations) did not significantly differ between the TriCurin and Vehicle-treated groups (Fig. 1k). This supported the possibility that TriCurin treatment causes suppression of M2 TAM and simultaneous activation/recruitment of a discrete population of M1 TAM [12].

TriCurin treatment causes suppression of P-STAT3 in the tumor-associated macrophages. C has been known to inhibit the ARG1-inducing transcription factor STAT3, which is a

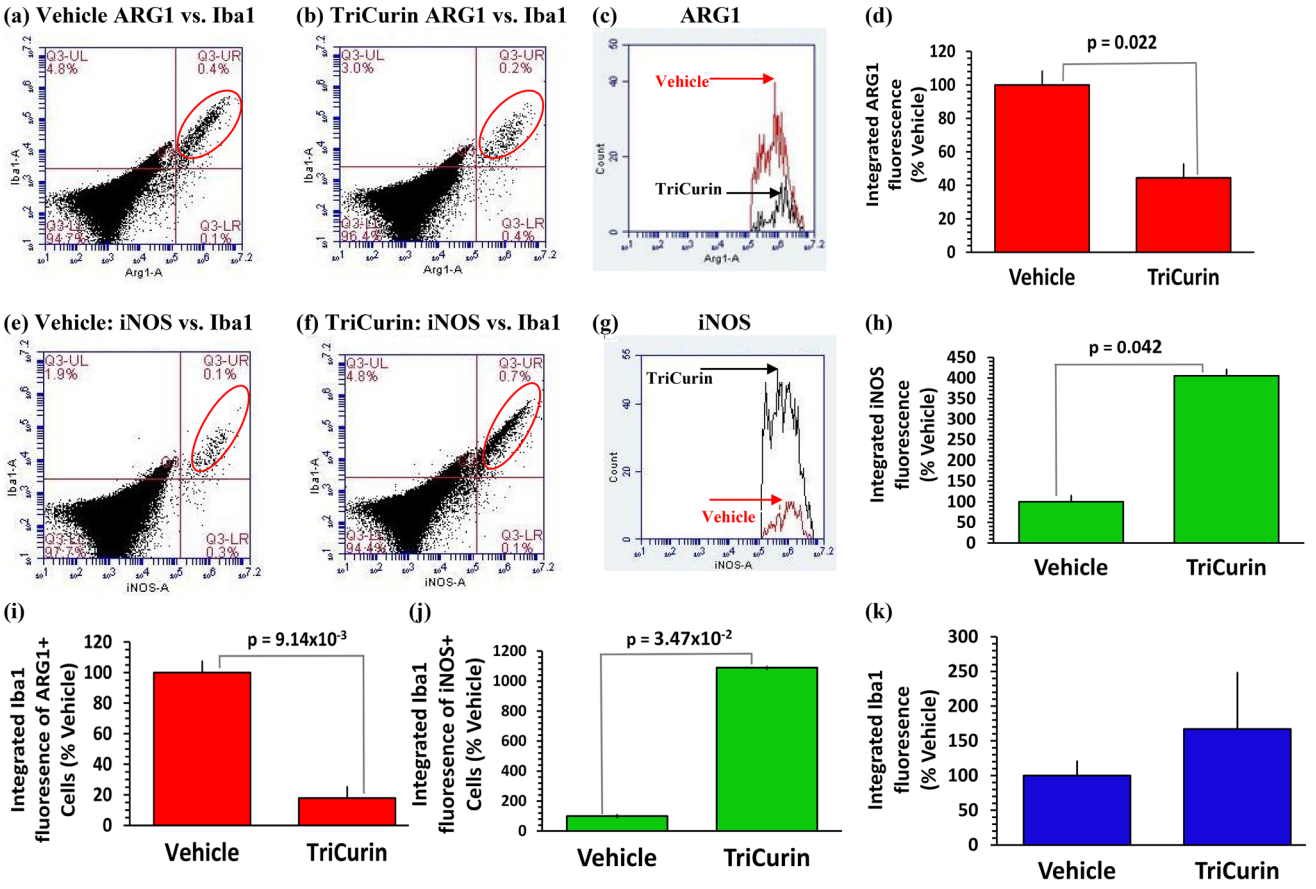

Fig. 1 Five days of TriCurin treatment causes repolarization of tumor-associated macrophages (TAM) from M2 to M1-type in TC-1 tumor. Cells from TC-1-implanted mice with 5 days of TriCurin or Vehicle (PBS) treatment (daily, see "Materials and methods") were dispersed, fixed, permeabilized, and immunostained using iNOS, ARG1, and Iba1 (marks activated macrophages) antibodies, and the stained cells analyzed by flow cytometry. **a–c** Integrated fluorescence intensity (IF) (fluorescence per event x total number of events in a segregated population) obtained from double-stained events (red ellipse, upper right (UR) quadrant) for ARG1 (green) and Iba1 (red) was considered and the IF profiles of ARG1+cells were obtained for both the groups. **e–g** Similarly, IF for iNOS+cells were obtained from both groups (Vehicle: red, TriCurin: black) values obtained from double-stained events [red ellipse, UR quadrant for iNOS (green) and Iba1 (red)]. **d, h** Graphs showing a 56% decrease in ARG1 IF ($p=0.022$) and a 305% increase in iNOS IF ($p=0.042$) (with respect to Vehicle-treated) using Vehicle-treated and TriCurin-treated mice (mean ± S.E.) ($n=4$ for each group). **i, j** Similarly, Iba1 IF quantified from **a, b, e**, and **f** shows a concomitant decrease in Iba1 integrated fluorescence in the ARG1+cells (80%) ($p=9.14\times10^{-3}$) and an increase in Iba1 integrated fluorescence (989%) in iNOS+cells ($p=0.035$) with respect to the Vehicle-treated for each group (mean ± SEM) ($n=4$ for each group). **k** No significant difference in Iba1 IF between double-positive cells from the Vehicle-treated and the TriCurin-treated groups

marker for the immunosuppressive M2-type TAM [13, 20, 27]. To understand if STAT3 was a major player in the TriCurin-mediated repolarization of Iba1+TAM (Supplementary Fig. 1) from M2 to M1-type, we performed immunohistochemistry of tumor sections from Vehicle and TriCurin groups for STAT3 and activated STAT3 (P-Y^{705}-STAT3, or P-STAT3). The M2 TAM in the Vehicle-treated TC-1 tumor harbored elevated levels of P-STAT3. In contrast, the M1 TAM in the TriCurin-treated tumors exhibited 80% suppression of P-STAT3 (Fig. 2a, b). A comparison with the corresponding total STAT3 levels revealed that the overall suppression of P-STAT3 was due to a combination of suppressed STAT3 expression (56% decrease) (Fig. 2a, c) and inhibited STAT3 phosphorylation (51% decrease) (Fig. 2a, d).

TriCurin treatment causes an induction in P-STAT1 and P-NF-KB (P-p65) in the TAM. STAT3 activation causes IL10-mediated suppression of the transcription factor STAT1 in the TAM [28]. Based on our previous results (Fig. 2), inhibition of STAT3 by TriCurin is expected to result in the activation of STAT1 [12], a transcription factor that triggers iNOS and IL12 synthesis in the TAM [29]. To investigate the activation status of STAT1 in both groups (Vehicle and TriCurin), we immunostained the TAM using antibodies against STAT1 and activated STAT1 (P-Tyr^{701}-STAT1). The Iba1+ cells in the Vehicle-treated mice showed

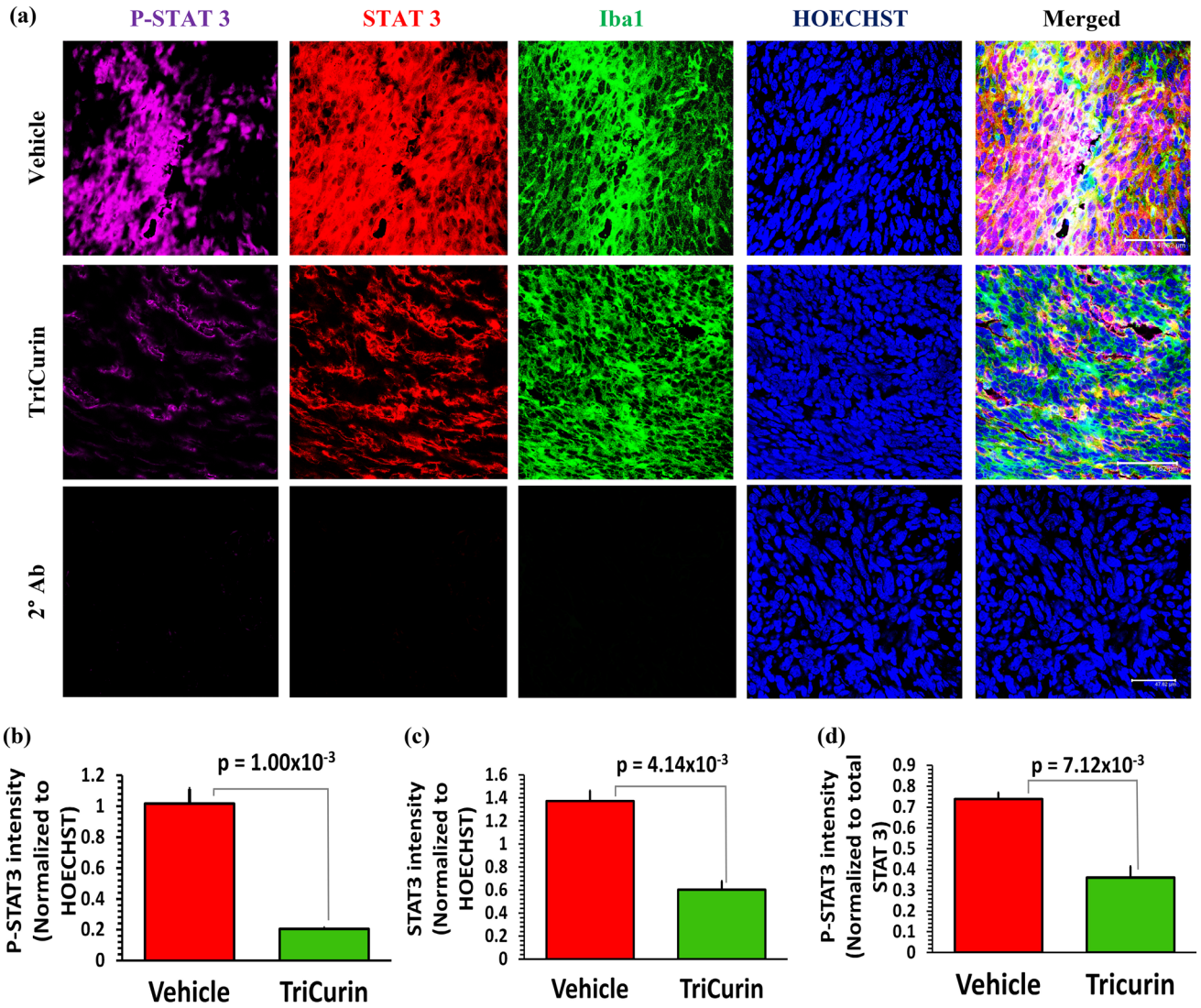

Fig. 2 Five days of TriCurin treatment causes a dramatic suppression of P-STAT3 in the tumor-associated macrophages (TAM). TC-1 tumor sections parallel to those used in Supplementary Fig. 1 were used to assess the levels of STAT3 and P-Tyr^{705}-STAT3 (activated) in the Iba1+ macrophages. **a**, upper and middle rows, and **b** the Vehicle-treated mice displayed a high level of activated STAT3 (P-Y^{705}-STAT3) in the TAM, which was suppressed by 80% ($p = 1.0 \times 10^{-3}$) in the TriCurin-treated group. This overall suppression of P-STAT3 was due to a combination of **c** suppression of STAT3 expression (STAT3 fluorescence normalized to HOECHST fluorescence) and **d** STAT3 activation (P-STAT3 normalized to STAT3). Four randomly chosen sections per mouse were used for imaging and the data (mean ± SEM) obtained from Vehicle-treated ($n = 4$) and TriCurin-treated ($n = 4$) groups. HOECHST = HOECHST33342. (Scale bar: 47.62 μm). **a**, lower row, absence of non-specific staining in sections treated with three 2° antibodies consecutive to one another (see "Materials and methods")

basal levels of activated STAT1, whereas the M1 TAM in the TriCurin-treated tumors exhibited a 532% increase in P-STAT1 (Fig. 3a, b). A comparison with the corresponding total STAT1 levels revealed that the overall increase in P-STAT1 was due to a combination of induced STAT1 expression (219% increase) (Fig. 3a, c) and increased STAT1 phosphorylation (activation) (97% increase) (Fig. 3a, d).

Activated NF-kB (p65) has been known to be overexpressed in M1 TAM [30]. In addition, earlier work in macrophages shows that co-activated NF-kB (p65) and STAT1 cooperate by binding to enhancer elements on the *iNOS* gene [12, 31, 32]. To effect such alterations in the tumor-associated macrophages, TriCurin treatment should cause simultaneous activation these two transcription factors. As expected, immunostaining of the TAM using antibodies against NF-kB (p65) and activated NF-kB p65 (P-Ser^{276}-p65) revealed a 2071% increase in P-p65 (P-NF-kB) in the TAM (Fig. 4a, b). A comparison with the corresponding total NF-kB (p65) levels revealed that the overall increase in P-p65 was due to a combination of induced NF-kB (p65)

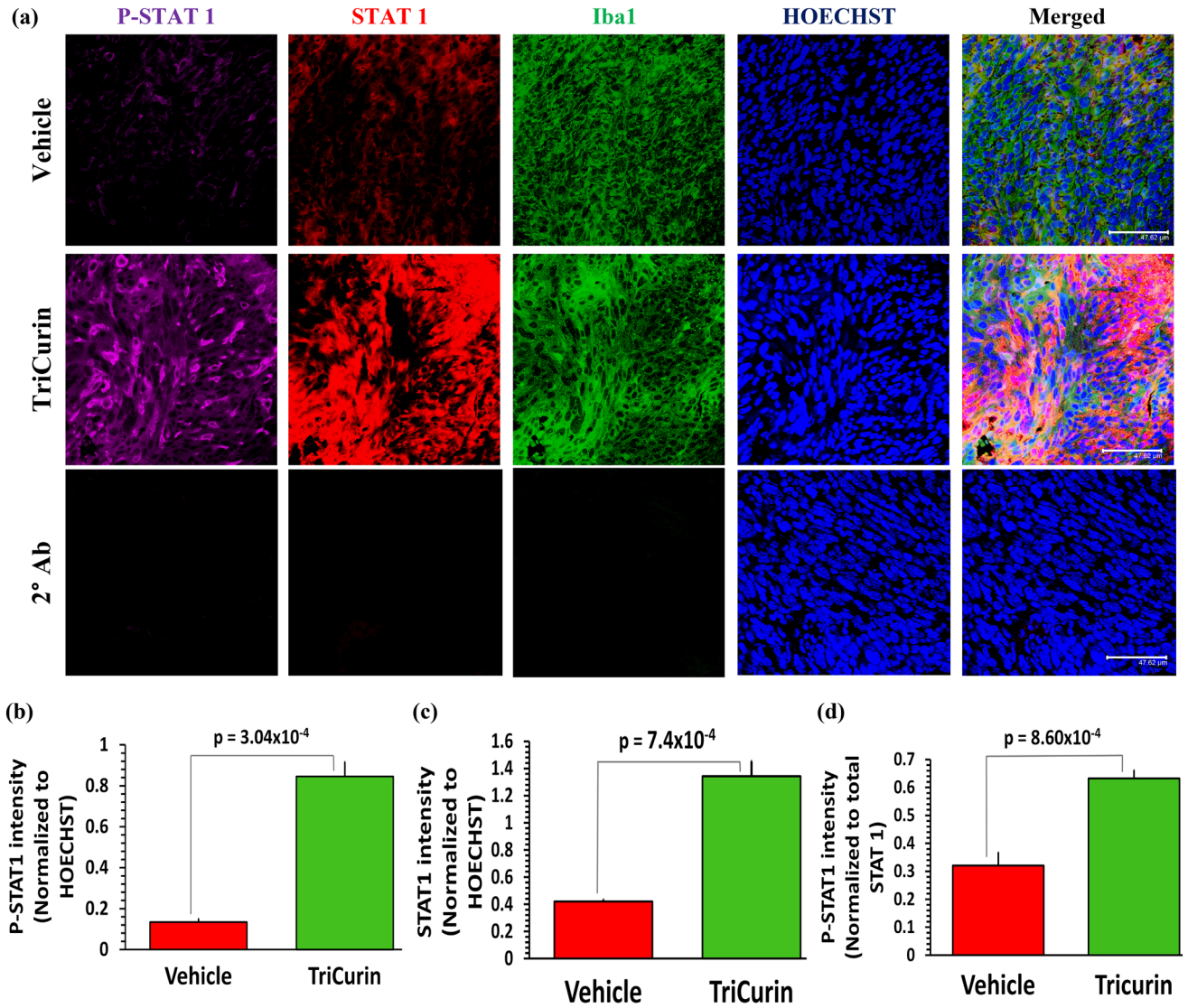

Fig. 3 TriCurin treatment causes an induction in P-STAT1 in the TAM. TC-1 tumor sections parallel to those used in Supplementary Fig. 1 were stained to determine the levels of STAT1 and P-Tyr^{701}-STAT1 (activated) in the tumors from Vehicle-treated and TriCurin-treated mice. **a** Upper and middle rows, and **b** the Vehicle-treated mice displayed basal levels of activated STAT1 (P-Tyr^{701}-STAT1) in the Iba1+TAM, which was increased by 532% ($p = 3.04 \times 10^{-4}$) in the TC-1 tumor sections from the TriCurin-treated group. This overall increase in P-STAT1 was due to a combination of (**c**) induction of STAT1 expression (STAT1 normalized to HOECHST) and **d** STAT1 activation (P-STAT1 normalized to STAT1). Four randomly chosen sections per mouse were used for imaging and the data (mean ± SEM) were compared between Vehicle-treated and TriCurin-treated groups ($n = 4$ per group). (Scale bar: 47.62 µm). (**a**, lower row) Absence of non-specific staining from the 2° antibodies (see "Materials and methods")

expression (226% increase) (Figs. 4a, 2c) and increased NF-kB (p65) phosphorylation (activation) (536% increase) (Figs. 4a, 2d).

Five days of TriCurin treatment is adquate to cause repolarization of IL12^{low}, IL10^{high} tumor-associated M2 macrophages to IL12^{high}, IL10^{low} M1-type in TC-1 tumor. Suppression of P-STAT3 is known to cause reduced IL10 (M2 TAM marker) expression along with increased IL12 (M1 TAM marker) expression [33]. Based on this understanding, we wanted to verify if the observed TriCurin-mediated M2→M1 polarization (Fig. 1) was associated with a switch in the Iba1+ TAM to IL12^{high} and IL10^{low} (M1) phenotype. As expected, tumors from the Vehicle-treated group had high IL10 and very low IL12 in the Iba1(+) TAM, whereas the TAM in tumor sections from the TriCurin-treated mice showed a 70% decrease in IL10 and a 244% increase in IL12 expression (Supplementary Fig. 2). This further demonstrated the TriCurin-evoked M2→M1 switch using a second set of markers for M2 and M1, IL10, and IL12, respectively.

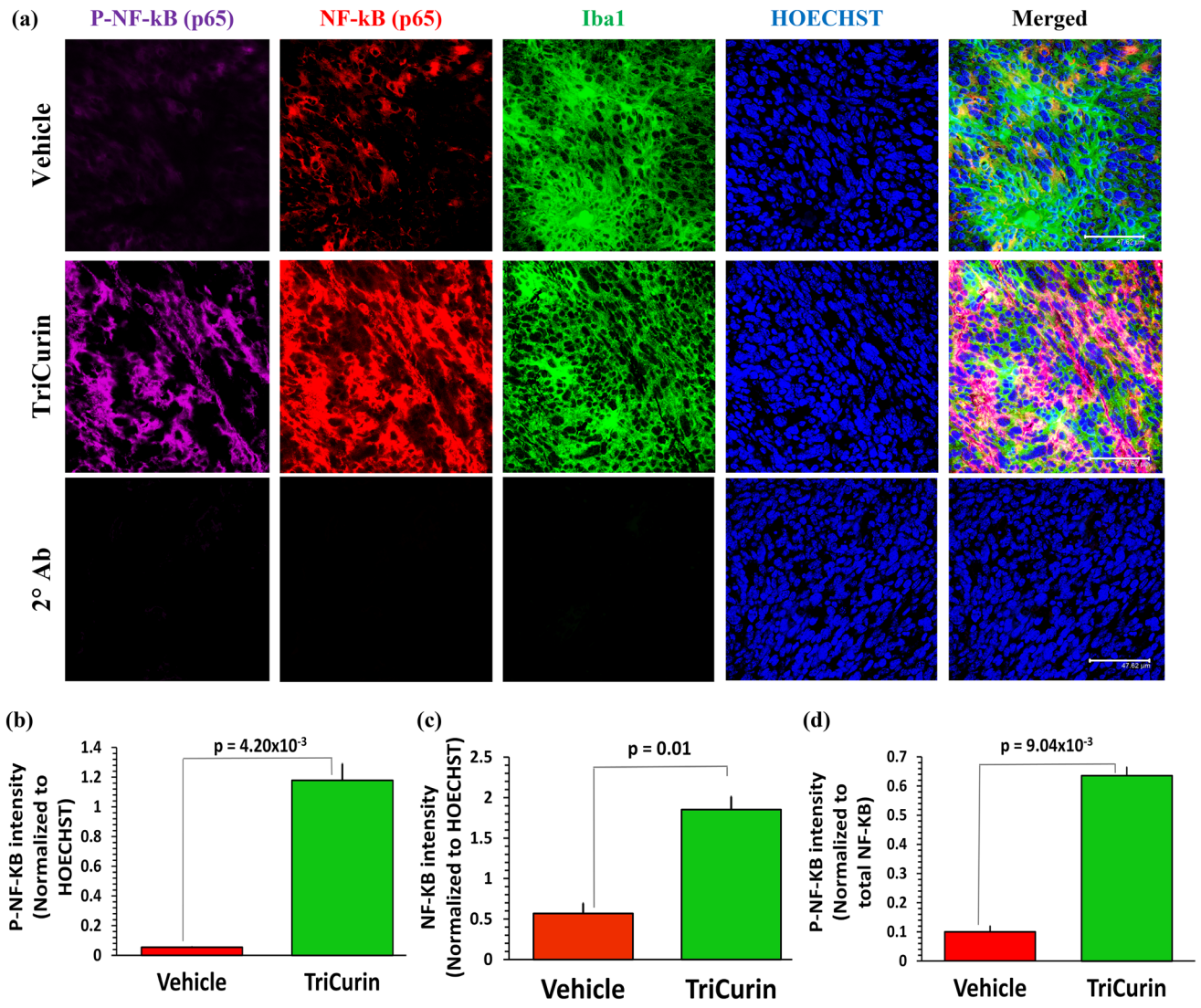

Fig. 4 TriCurin treatment causes an induction in P-NF-KB (P-p65) in the TAM. TC-1 tumor sections parallel to those used in Supplementary Fig. 1 were stained to determine the levels of NF-kB (p65) and activated NF-kB p65 (P-Ser^{276}-p65) in the tumors from Vehicle-treated and TriCurin-treated mice. **a** Upper and middle rows and **b** the Vehicle-treated mice displayed basal levels of activated NF-kB p65 (P-Ser^{276}-p65) in the iba1+TAM, which was increased by 2071% in the TriCurin-treated TC-1 tumor sections ($p = 4.20 \times 10^{-3}$). This overall increase of P-NF-kB (P-p65) was a result of **c** induction of NF-kB (p65) expression (NF-kB (p65) normalized to HOECHST) and **d** NF-kB (p65) activation (P-NF-kB (P-p65) normalized to NF-kB (p65)). Four randomly chosen sections per mouse were used for imaging and the data (mean ± SEM) compared between Vehicle-treated and TriCurin-treated groups ($n = 4$ per group). (Scale bar: 47.62 µm). **a** lower row, showed the lack of non-specific staining from the secondary antibodies (see "Materials and methods")

IL12 is known to trigger intra-tumor recruitment of activated NK cells and cytotoxic T lymphocytes [21, 29, 34–37]. To verify the role of IL12 in causing recruitment of NK cells and CTL that would cause enhanced elimination of tumors, we neutralized the IL12 receptor-mediated signaling in these immune cells by peripheral treatment with IL12p40 antibody [24, 29].

IL12Ab treatment abrogates TriCurin-evoked infiltration of natural killer (NK) cells into TC-1 tumors. C has also been reported to activate NK cells in tumors [16]. Cognizant of these studies, we investigated the possibility of TriCurin-evoked, intra-tumor recruitment of activated NK cells (in addition to M1 TAM polarization) as a mechanism for its anti-tumor activity [21]. Based on flow cytometry data from Vehicle, TriCurin, and TriCurin + IL12Ab groups, TriCurin evoked a 376% increase in infiltrating activated (NKp46+) NK cells, which was eliminated in the TriCurin + IL12Ab group NKp46+ fluorescence (UL quadrant. red ellipse) within the tumor, thus confirming infiltration of NK cells into the TC-1 tumors in response to TriCurin treatment (Fig. 5a–e). Furthermore, based on immunohistochemical data, the 5-day treatment with TriCurin caused

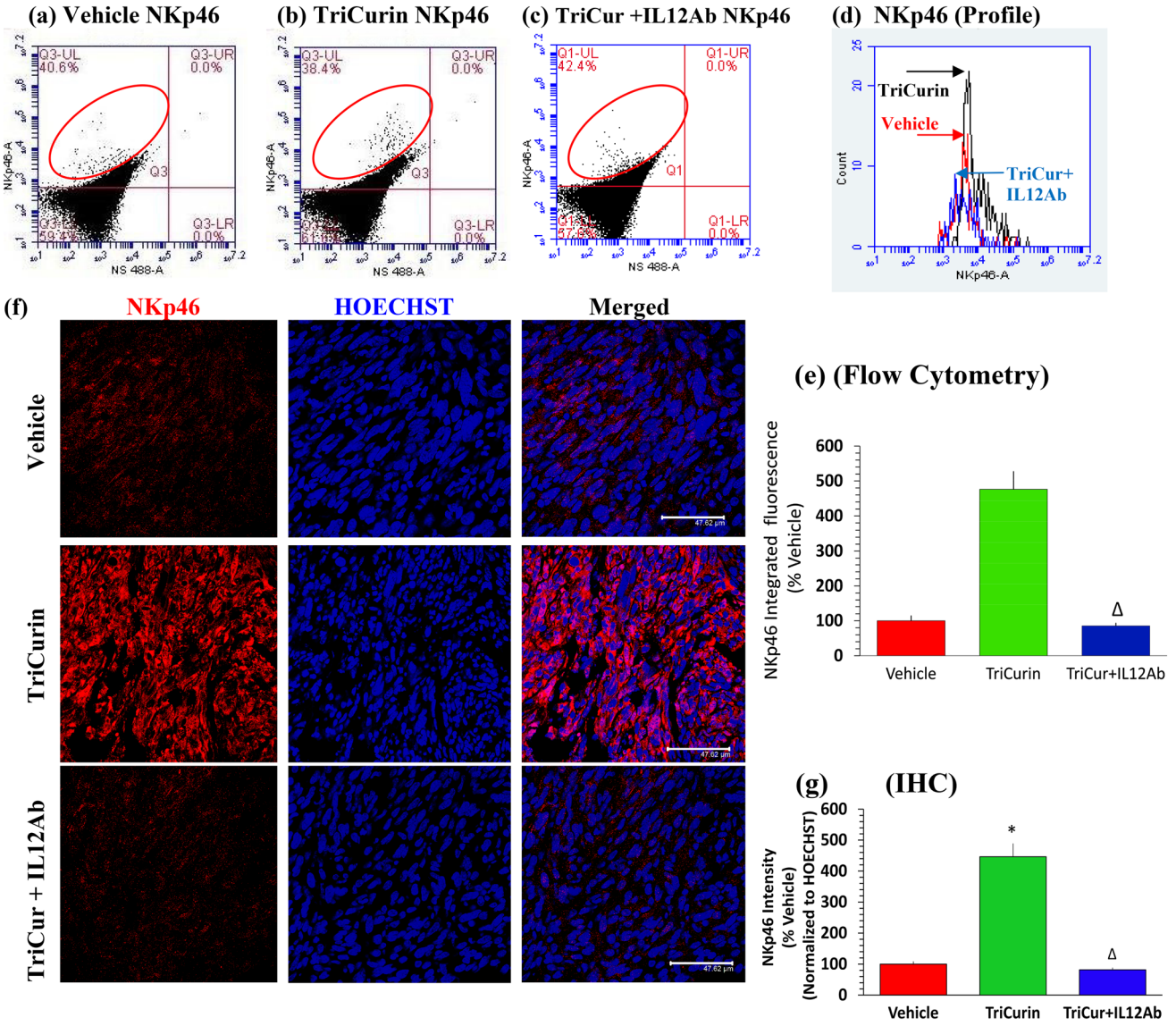

Fig. 5 IL12 Ab treatment abrogate infiltration of natural killer (NK) cells into TC-1 tumors. Cells from TC-1 tumor implanted mice with 5-day TriCurin (plus normal rat serum, see "Materials and methods"), TriCurin + IL12Ab and Vehicle (PBS) treatments were dispersed, fixed, and permeabilized, the cells immunostained using the activated NK cell-specific NKp46 antibody, and then analyzed by flow cytometry. **a–d** IF from single-stained NKp46+ events (red ellipse, UL quadrant) was considered from the three groups, expressed as mean ± S.E. (Vehicle: red, TriCurin: black, TriCurin + IL12Ab: blue) (Vehicle, $n=4$; TriCurin, $n=4$; TriCurin + IL12Ab, $n=3$). **a, b, d, e** TriCurin treatment affords a 376% increase in NKp46 IF (with respect to Vehicle-treated, $^*p=0.019$). **a, c, d, e** TriCurin + IL12Ab displayed an NKp46 IF, which was comparable to that of the Vehicle group (with respect to TriCurin-treated, $\Delta p=0.02$). **f** upper, middle, and lower rows, and **g** TC-1 tumor sections from Vehicle-, TriCurin-, and TriCurin + IL12Ab-treated mice were single-stained with the NKp46 antibody. The Vehicle-treated tumor tissue displayed minimal NKp46 fluorescence, but the TriCurin-treated mice showed a 346% increase in NKp46-staining (with respect to the Vehicle), confirming the recruitment of activated NK cells ($^*p=1.25\times10^{-3}$).TriCurin + IL12Ab treatment reversed this recruitment of NKp46+ NK cells to the level in the Vehicle group (with respect to TriCurin-treated, $\Delta p=1.0\times10^{-3}$). Four randomly chosen sections per mouse were used for imaging and the data obtained were expressed as (mean ± S.E.M.), from Vehicle-treated ($n=4$), TriCurin-treated ($n=4$), and TriCurin + IL12Ab ($n=3$) groups. (Scale bar: 47.62 µm)

a 346% increase in activated (NKp46+) NK cells in the TC-1 tumors (Fig. 5f, g) [38]. In contrast, infiltration of activated (NKp46+) NK cells was virtually eliminated in the TriCurin + IL12Ab group, thus confirming the role of TriCurin-induced IL12 (Supplementary Fig. 2) in causing this intra-tumor recruitment of activated NK cells (Fig. 5f, g). Interestingly, C is also known to cause enhanced expression of IFNγ from tumor-associated immune cells (lymphocytes like NK cells and CTL), which, in the case of TriCurin, could prolong the M1 TAM phenotype [17, 19, 29, 34, 38].

IL12 Ab treatment eliminates TriCurin-evoked infiltration of Cytotoxic T lymphocytes into TC-1 tumors. CTL are known to be highly tumoricidal and C has been known to promote intra-tumor infiltration of activated CD8+ CTL to cause tumor elimination [17, 19, 20]. In addition, M1-macrophage-derived IL12 has been known to promote the activation and infiltration of CTL [35–37]. Therefore, we next investigated if TriCurin treatment was capable of causing intra-tumor infiltration of activated CD8+ CTL and if IL12 regulated this process (Supplementary Fig. 2). As revealed by immunohistochemistry for CD8+ CTL, the 5-day treatment with TriCurin triggered a 633% increase in activated (CD8+) CTL in the TC-1 tumors (Supplementary Fig. 3a, b). In addition, data from the TriCurin + IL12Ab group revealed the lack of tumor-infiltrating activated (CD8+) CTL, despite TriCurin treatment, thereby indicating that the IL12 plays a major role in causing the intra-tumor recruitment of activated CTL (Supplementary Fig. 3a, b).

IL12 Ab treatment partially reverses TriCurin-induced apoptosis of E6+ tumor cells and tumor size reduction. In our prior studies, intra-tumor injection of TriCurin into HaRas+, HPV16 E6+, and E7+ TC-1 cell-implanted mice, every 72 h for 10 days caused an 80–90% decrease in tumor growth [8]. Here, we examined if the onco-immunotherapeutic effect of TriCurin in recruiting/activating M1 TAM, NK cells, and CTL in 5 days was also associated with a concomitant reduction in tumor load. Furthermore, we asked if neutralization of NK cells and CTL by IL12 Ab infusion influences the effect of TriCurin [21, 29, 34–37]. Five days of intra-tumor TriCurin infusion (every 24 h) caused a 61% decrease in tumor growth, whereas application of IL12 antibody (i.p.) along with TriCurin (intra-tumor) caused a partial reversal of the TriCurin-triggered inhibition of tumor growth (41% decrease) (tumor volumes were determined using water displacement) (Fig. 6a, b). Based on flow cytometry, the reduction in tumor load was associated with a flow cytometry analysis which showed a 68% inhibition of E6 expression in these tumor cells (LR quadrant: red ellipse) (Fig. 6c, d, f, g). The TriCurin + IL12Ab group showed only a 38% inhibition of E6 in these tumor cells, verifying that the neutralization of NK cells and CTL causes 30% less elimination of these tumor cells by (Fig. 6c, e–g). Based on immunohistochemistry, the tumor load reduction was concomitant with an inhibition of the oncoprotein E6 (54% decrease) (Fig. 6h, i) and activation of caspase 3 (383% increase) (Fig. 6h, j) in the tumor cells. In contrast, the TriCurin + IL12Ab group revealed a 31% inhibition of the oncoprotein E6 (Fig. 6h, i) and 67% increase in active-caspase 3 (Fig. 6h, j). Thus, neutralization of NK cells and CTL with the IL12Ab impacted tumor elimination by causing 23% less inhibition of E6 and 316% less activation of caspase 3. This is consistent with our previous in vitro observation that TriCurin treatment for 6 h causes suppression of E6, increased acetylation-mediated activation of p53, and elevation of active-caspase 3 in cultured TC-1 cells [8].

Prolonged TriCurin treatment triggers P-NF-kB and P-STAT1-mediated M2 to M1 polarization of TAM, recruitment of activated NK cells, and suppression of E6+ cells in HNSCC xenograft tumors. To translate the novel findings from our TC-1 model into a more clinically relevant human tumor model, HPV16+ HNSCC cells UMSCC47 were implanted into the flanks of athymic *nude/nude* (NCr) mice (xenograft model); and after the tumors were palpable, the immuno-modulatory effect of intra-tumor TriCurin injection for 5 weeks (3 doses per week) was assessed [7].

Immunohistochemical analysis revealed that the Vehicle-treated TAM were $iNOS^{low}$, $ARG1^{high}$, and Iba1+ M2 macrophages. In contrast, similar to the 5-day treatment, prolonged TriCurin treatment also caused a major shift in polarity of the Iba1+ TAM to the $iNOS^{high}$, $ARG1^{low}$ M1 form (Supplementary Fig. 4a). We observed an 89% decrease in ARG1 (Supplementary Fig. 4a, b) and a 684% increase in iNOS (integrated fluorescence) (Supplementary Fig. 4a, c).

Our previous results (Fig. 2) and other reports have shown that both TriCurin as well as C are a potent suppressors of activated STAT3 in M2 TAM and that STAT3 suppression causes activation of STAT1, leading to the formation of the M1 phenotype [13, 28]. Also the findings from our TriCurin-treated TC-1 tumors (Figs. 3, 4) and other reports have revealed that the co-activated transcription factors STAT1 and NF-kB (p65) are likely to trigger the expression of the M1-linked enzyme iNOS, which produces NO that is known to cause tumor elimination [12, 13, 26, 30–32]. Immunohistochemical analysis of the Iba1+ TAM in the TriCurin-treated HNSCC-implanted xenograft tumors revealed elevated levels of co-localized, P-STAT1 (993% increase), and activated P-p65 (93% increase) in the TriCurin-treated Iba1+ TAM (Supplementary Fig. 5a–c).

Given the evidence of interaction between M1 TAM and activated NK cells in the tumor microenvironment (Supplementary Fig. 2, Figs. 5, 6), we also probed for tumor-infiltrating activated NK cells in these xenograft tumors [29, 34, 39]. Immunostaining revealed elevated levels of intra-tumor NKp46+ NK cells (441% increase) in the TriCurin-treated tumors (Supplementary Fig. 6a–b). This recruitment of activated NK cells is expected to result in stabilization of the M1 TAM phenotype, thereby causing elimination of tumors by the coordinated action of TAM and NK cells [19, 21, 29, 38, 40]. As expected, the intra-tumor activation/recruitment of M1 TAM and NK cells was associated with the suppression in E6+ tumor cells (Supplementary Fig. 6a) and an 86% reduction in tumor size, as reported earlier [7]. These results were consistent with our previously reported

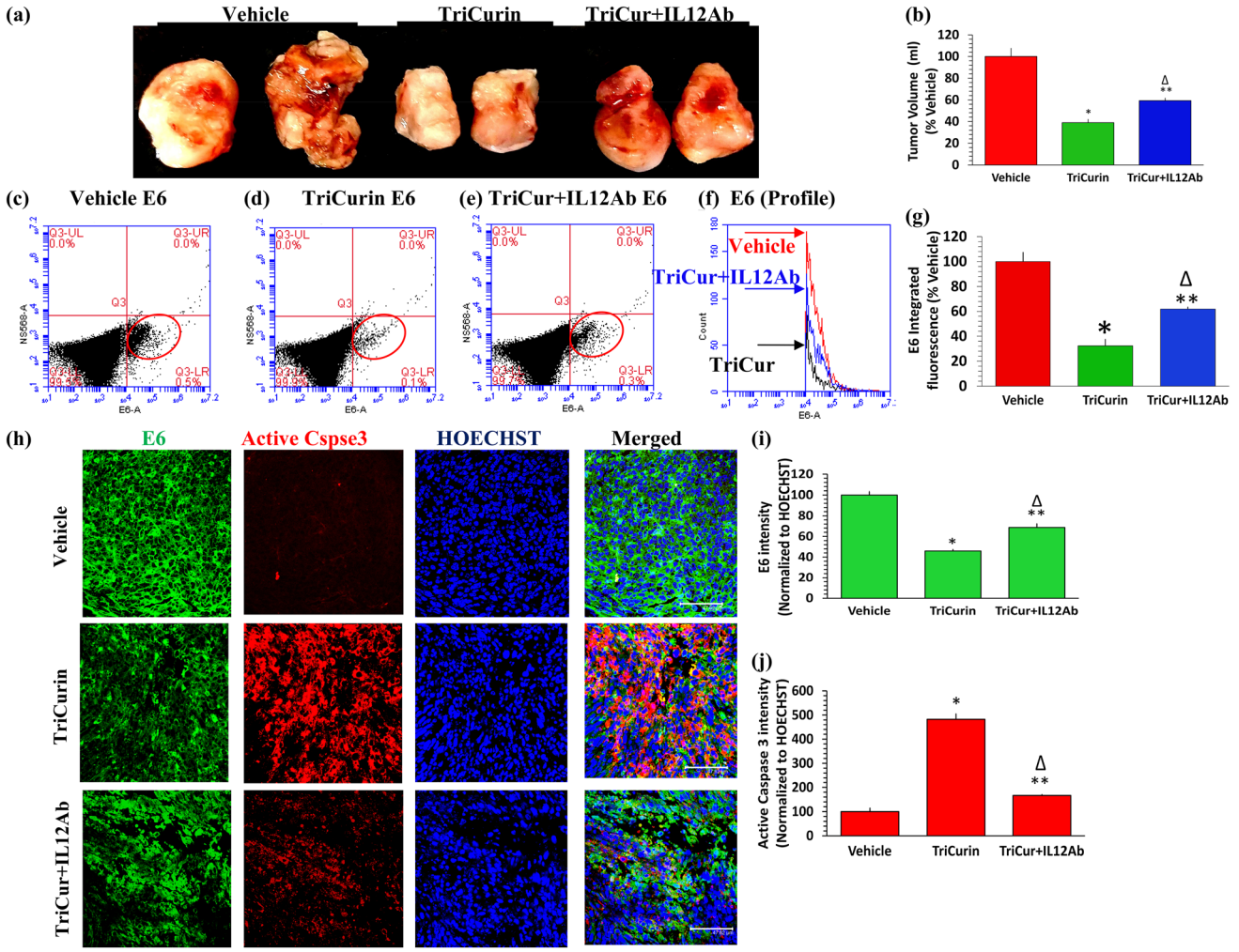

Fig. 6 IL12Ab treatment partially reverses TriCurin-induced apoptosis of E6+tumor cells and reduction in tumor load. **a** Volumes of extricated tumors from Vehicle (PBS)-treated, TriCurin-treated, and TriCurin+IL12Ab-treated mice were measured by the water displacement on the day of sacrifice (day 6). Two representative tumors from each group are shown here. **b** Even after the 5-day treatment, the TriCurin group (six mice per group) showed a dramatic decrease in tumor size (61% relative to Vehicle-treated) ($n=6$) ($^{*}p=2.54\times10^{-5}$). The TriCurin+IL12Ab group ($n=3$) exhibited a smaller decrease in tumor size (41% relative to Vehicle-treated, $^{**}p=8.4\times10^{-3}$) ($\Delta p=5.8\times10^{-3}$ relative to TriCurin-treated) (mean ± S.E.M). **c–f** Tumor cells from 5 days of TriCurin, TriCurin+IL12Ab, and Vehicle treatment were dispersed, fixed, permeabilized, immunostained using the HPV+tumor cell-specific E6 antibody, and analyzed by flow cytometry. IF from single-stained E6+events (red ellipse, LR quadrant) was obtained from the three groups (Vehicle: red, TriCurin: black, TriCurin+IL12Ab: Blue). **g** Relative to the Vehicle group ($n=5$), the TriCurin group ($n=5$) showed a 68% decrease in E6 IF ($^{*}p=0.01$) and the TriCurin+IL12Ab-treated mice ($n=3$) showed a 38% decrease in E6 IF ($^{**}p=0.04$) ($\Delta p=0.02$ relative to TriCurin-treated), **h** upper, middle, and lower rows, **i** and **j** tumor sections from these three groups also were subjected to immunohistochemistry to assess caspase 3 (Cspse3) activation and E6 expression. The Vehicle group showed high E6 expression (green) and negligible active-caspase 3 (red). Relative to the Vehicle group, the TriCurin group showed a 54% suppression of E6 ($^{*}p=1.2\times10^{-3}$) (**i**) and a sharp increase in active-caspase 3 (383% increase) ($^{*}p=4.0\times10^{-4}$) (**j**). Relative Vehicle-treated, the TriCurin+IL12Ab group showed only 31% suppression of E6 ($^{**}p=8.8\times10^{-3}$) ($\Delta p=0.03$ relative to TriCurin-treated) (**i**). Relative to Vehicle-treated, the TriCurin+IL12Ab group showed 67% upregulation of active-caspase 3 upregulation ($^{**}p=0.04$) ($\Delta p=2\times10^{-3}$ relative to TriCurin-treated) (**j**). Four randomly chosen sections per mouse were used for imaging and data quantified from Vehicle-treated ($n=4$), TriCurin-treated ($n=4$) and, TriCurin+IL12Ab-treated ($n=3$) groups. (Scale bar: 47.62 µm)

in vitro data showing suppression of E6, increase in p53 levels, and induction of apoptosis in HNSCC cells following TriCurin treatment [7].

Discussion

This project involved intra-tumor injection of TriCurin, which is expected to cause direct apoptosis of a number of tumor cells. However, due to rapid degradation

of C in vivo, the concentration of TriCurin-derived C in the body is expected to drop quickly. Interestingly, our in vivo pharmacokinetic studies [Mukherjee et al., unpublished] using a lipid-encapsulated formulation of TriCurin yielded plasma concentrations of C in the nano-molar range (610–210 nM), which is not high enough to directly kill TC-1 and UMSCC47 cells, as the IC50 values of TriCurin for these cells are much higher (13 μM+ and 3.22 μM+, respectively) [7, 8]. Based on our observation that injected TriCurin causes a dramatic reduction in tumor load, we expect that in addition to eliciting direct tumor cell death immediately after intra-tumor injection, TriCurin would elicit its anti-tumor activity also by stimulating the immune cells, which are known to eliminate tumors [12, 13, 16, 19, 20, 41]. Our current study tests this postulate by demonstrating that TriCurin, indeed, causes intra-tumor recruitment of M1 TAM, NK cells, and CTL which are known to eliminate tumor cells [21, 26, 29, 30, 38].

Our data show that TriCurin treatment causes activation/recruitment of M1 TAM, NK cells, and CTL into pre-clinical HPV+ cervical (TC-1 implanted mice) and activation/recruitment of M1 TAM and NK cells in HNSCC (xenograft) tumors (Fig. 6) [7]. Analysis of these TriCurin-treated tumors (Fig. 1, Supplementary Fig. 2 and Supplementary Fig. 4) reveals a major shift in polarity of $ARG1^{high}$, $iNOS^{low}$, $IL10^{high}$, $IL12^{low}$ M2 TAM into the $ARG1^{low}$. $iNOS^{high}$, $IL10^{low}$, and $IL12l^{high}$ M1-type [12]. This repolarization is concomitant with repression of activated STAT3 and induction of activated STAT1 and NF-kB (p65) in the TAM (Figs. 2, 3, 4 and Supplementary Fig. 5). Activated STAT1 is known to cooperate with activated NF-kB (p65) to trigger the M1 phenotype, which is marked by the induction of IL12 and iNOS which should trigger toxic NO production by the TAM (Fig. 1, Supplementary Fig. 2, and Supplementary Fig. 4) [12, 13, 28, 30–32]. We also demonstrate TriCurin-mediated, intra-tumor recruitment of activated NK cells and CTL (Fig. 5, Supplementary Fig. 3, and Supplementary Fig. 6), which are expected to contribute to the observed tumor load reduction (Fig. 6 and Supplementary Fig. 6) [7, 16, 21]. The IL12-mediated NK cell and CTL recruitment and activation are attenuated in mice pretreated with an IL12-neutralizing antibody (Supplementary Fig. 2, Supplementary Fig. 3, and Fig. 5). This recruitment of CTL and NK cells may simultaneously cause IFNγ-mediated observed stimulation of STAT1 in macrophages and M1-type polarization of TAM, thereby enabling the activated NK cells, CTL, and the M1 TAM to act as a lethal triad against cancer cells. Corroboratively, IL12Ab-mediated abrogation of intra-tumor recruitment of activated NK cells and CTL partially eliminated the tumoricidal activity of TriCurin (Fig. 6) [13, 16, 19, 21, 29, 33, 34, 36, 38, 40].

Our data also indicate that TriCurin causes this shift in polarity by silencing the M2 TAM and activating/recruiting a discrete population of M1 TAM while maintaining a constant number of overall intra-tumor Iba1+ TAM (Fig. 1i, j, k) [12]. Interestingly, NKp46+ NK cells have been reported to eliminate M2 macrophages while causing IFNγ-mediated activation and amplification of MHC class I^{high} M1 macrophages [42]. Based on the previous findings of other groups and the data presented in this manuscript, we propose a working model in which injected TriCurin elicits a switch in TAM phenotype from a tumor-promoting M2-type into a tumoricidal M1-type. Furthermore, founded on our IL12 blocking data, we postulate that TriCurin-induced M1 TAM-derived IL12 is responsible for triggering intra-tumor recruitment of NK cells and CTL and elimination of the HPV+ cervical cancer cells (Fig. 6) [7, 8].

Treatments for HNSCC include chemotherapy and/or radiation, which are fairly toxic to the body and they deplete the tumoricidal immune cells [5, 6, 43]. Cancer immunotherapy using chimeric antigen receptor (CAR) T-cell treatment and regulators of T-cell activation (checkpoint inhibitors) has recently come into prominence but with limitations and side effects [22, 23]. Thus, there is an acute need for novel immunotherapeutic strategies to better manage the growing number of HPV+ tumors. TriCurin is highly efficient in stimulating the immune system against cancer cells and can be used as a safe immunotherapeutic agent to turn the immune system against HPV+ tumors.

Acknowledgements Sumit Mukherjee was supported by a teaching assistantship from the College of Staten Island (CUNY).

Author contributions PB, SM, QP, and LP conceived and planned the experiments. SM, RH, RW, DA, AF, SS, and LP carried out the experiments. All the authors contributed to the interpretation of results. SM and PB took the lead in writing the manuscript. All authors provided critical feedback and helped in shaping the final manuscript.

Funding This project was supported by Professional Staff Congress (PSC)-CUNY Grants from cycles 45 and 47.

Compliance with ethical standards

Conflict of interest Probal Banerjee has a pending patent application "Activity Enhancing Curcumin Compositions and Methods of Use", PCT/US14/67819 pending. The remaining authors declare no conflict of interest.

Ethical approval and ethical standards All procedures performed in studies involving animals were in accordance with the ethical standards of the Institutional Animal Care Committees (IACUC) at the College of Staten Island (approval # 11 – 008) and The Ohio State University Medical Center (approval # 2009A0172).

Animal source Adult C57BL/6 female mice (2–6 months old) used for the TC-1 tumor experiments were bred and handled at the College of Staten Island (CUNY) [8]. Athymic nude (NCr) mice were purchased from Charles River Laboratories (Wilmington, MA) for the Head and Neck Squamous Cell Carcinoma (HNSCC) UMSCC47 tumor xenograft model and housed at The Ohio State University animal facility

[7]. Both the strains mentioned above were bred and handled in accordance to the consent of respective Institutional Animal Care Committees (IACUC) at the College of Staten Island and The Ohio State University Medical Center. All animal protocols were approved by the respective Institutional Animal Care Committees (IACUC) at the College of Staten Island and The Ohio State University Medical Center.

References

1. Jemal A, Bray F, Center MM, Ferlay J, Ward E, Forman D (2011) Global cancer statistics CA. Cancer J Clin 61:69–90
2. Kamangar F, Dores GM, Anderson WF (2006) Patterns of cancer incidence, mortality, and prevalence across five continents: defining priorities to reduce cancer disparities in different geographic regions of the world. J Clin Oncol 24:2137–2150. https://doi.org/10.1200/jco.2005.05.2308
3. Fowler RS (2000) Vulvar vestibulitis: response to hypocontactant vulvar therapy. J Low Genit Tract Dis 4:200–203
4. Stanley M (2010) Potential mechanisms for HPV vaccine-induced long-term protection. Gynecol Oncol 118:2–7. https://doi.org/10.1016/j.ygyno.2010.04.002
5. Leemans CR, Braakhuis BJM, Brakenhoff RH (2011) The molecular biology of head and neck cancer. Nat Rev Cancer 11:9–22. https://doi.org/10.1038/nrc2982
6. Mirghani H, Amen F, Blanchard P, Moreau F, Guigay J, Hartl DM, Lacau St Guily J (2015) Treatment de-escalation in HPV-positive oropharyngeal carcinoma: ongoing trials, critical issues and perspectives. Int J Cancer 136:1494–1503. https://doi.org/10.1002/ijc.28847
7. Piao L, Mukherjee S, Chang Q et al (2017) TriCurin, a novel formulation of curcumin, epicatechin gallate, and resveratrol, inhibits the tumorigenicity of human papillomavirus-positive head and neck squamous cell carcinoma. Oncotarget 8:60025–60035. https://doi.org/10.18632/oncotarget.10620
8. Mukherjee S, Debata PR, Hussaini R et al (2017) Unique synergistic formulation of curcumin, epicatechin gallate and resveratrol, tricurin, suppresses HPV E6, eliminates HPV+ cancer cells, and inhibits tumor progression. Oncotarget 8:60904–60916. https://doi.org/10.18632/oncotarget.16648
9. Anand P, Kunnumakkara AB, Newman RA, Aggarwal BB (2007) Bioavailability of curcumin: problems and promises. Mol Pharm 4:807–818. https://doi.org/10.1021/mp700113r
10. Langone P, Debata PR, Dolai S, Curcio GM, Inigo JD, Raja K, Banerjee P (2012) Coupling to a cancer cell-specific antibody potentiates tumoricidal properties of curcumin. Int J Cancer 131:E569–E578. https://doi.org/10.1002/ijc.26479
11. Langone P, Debata PR, Inigo JDR, Dolai S, Mukherjee S, Halat P, Mastroianni K, Curcio GM, Castellanos MR, Raja K, Banerjee P (2014) Coupling to a glioblastoma-directed antibody potentiates anti-tumor activity of curcumin. Int J Cancer 135:710–719
12. Mukherjee S, Baidoo J, Fried A, Atwi D, Dolai S, Boockvar J, Symons M, Ruggieri R, Raja K, Banerjee P (2016) Curcumin changes the polarity of tumor-associated microglia and eliminates glioblastoma. Int J Cancer 139:2838–2849. https://doi.org/10.1002/ijc.30398
13. Zhang X, Tian W, Cai X, Wang X, Dang X, Dang W, Tang H, Cao H, Wang L, Chen T (2013) Hydrazinocurcumin encapsuled nanoparticles "Re-Educate" tumor-associated macrophages and exhibit anti-tumor effects on breast cancer following STAT3 suppression. PLoS One 8:e65896
14. Debata PR, Castellanos MR, Fata JE, Baggett S, Rajupet S, Szerszen A, Begum S, Mata A, Murty VV, Opitz LM, Banerjee P (2013) A novel curcumin-based vaginal cream Vacurin selectively eliminates apposed himan cervical cancer cells. Gynecol Oncol. 129:145–153
15. Purkayastha S, Berliner A, Fernando SS, Ranasinghe B, Ray I, Tariq H, Banerjee P (2009) Curcumin blocks brain tumor formation. Brain Res 1266:130–138. https://doi.org/10.1016/j.brainres.2009.01.066
16. Zhang HG, Kim H, Liu C, Yu S, Wang J, Grizzle WE, Kimberly RP, Barnes S (2007) Curcumin reverses breast tumor exosomes mediated immune suppression of NK cell tumor cytotoxicity. Biochim Biophys Acta 1773:1116–1123. https://doi.org/10.1016/j.bbamcr.2007.04.015
17. Bhattacharyya S, Md Sakib Hossain D, Mohanty S et al. (2010) Curcumin reverses T cell-mediated adaptive immune dysfunctions in tumor-bearing hosts. Cell Mol Immunol 7:306–315. https://doi.org/10.1038/cmi.2010.11
18. Chang YF, Chuang HY, Hsu CH, Liu RS, Gambhir SS, Hwang JJ (2012) Immunomodulation of curcumin on adoptive therapy with T cell functional imaging in mice. Cancer Prev Res (Phila.) 5:444–452. https://doi.org/10.1158/1940-6207.capr-11-0308
19. Luo F, Song X, Zhang Y, Chu Y (2011) Low-dose curcumin leads to the inhibition of tumor growth via enhancing CTL-mediated antitumor immunity. Int Immunopharmacol 11:1234–1240. https://doi.org/10.1016/j.intimp.2011.04.002
20. Lu Y, Miao L, Wang Y, Xu Z, Zhao Y, Shen Y, Xiang G, Huang L (2016) Curcumin micelles remodel tumor microenvironment and enhance vaccine activity in an advanced melanoma model. Mol Ther 24:364–374. https://doi.org/10.1038/mt.2015.165
21. Farag SS, Caligiuri MA (2006) Human natural killer cell development and biology. Blood Rev 20:123–137. https://doi.org/10.1016/j.blre.2005.10.001
22. Postow MA, Callahan MK, Wolchok JD (2015) Immune checkpoint blockade in cancer therapy. J Clin Oncol 33:1974–1982. https://doi.org/10.1200/JCO.2014.59.4358
23. Zhang H, Ye Z-l, Yuan Z-G, Luo Z-Q, Jin H-J, Qian Q-J (2016) New strategies for the treatment of solid tumors with CAR-T Cells. Int J Biol Sci 12:718–729. https://doi.org/10.7150/ijbs.14405
24. Scharton-Kersten T, Afonso L, Wysocka M, Trinchieri G, Scott P (1995) IL-12 is required for natural killer cell activation and subsequent T helper 1 cell development in experimental leishmaniasis. J Immunol 154:5320–5330
25. Huang Z, Peng S, Knoff J, Lee SY, Yang B, Wu T-C, Hung C-F (2015) Combination of proteasome and HDAC inhibitor enhances HPV16 E7-specific CD8+ T cell immune response and antitumor effects in a preclinical cervical cancer model. J Biomed Sci 22:7
26. Brantley EC, Guo L, Zhang C, Lin Q, Yokoi K, Langley RR, Kruzel E, Maya M, Kim SW, Kim S-J, Fan D, Fidler IJ (2010) Nitric oxide-mediated tumoricidal activity of murine microglial cells. Transl Oncol 3:380–388
27. Chakravarti N, Myers JN, Aggarwal BB (2006) Targeting constitutive and interleukin-6-inducible signal transducers and activators of transcription 3 pathway in head and neck squamous cell carcinoma cells by curcumin (diferuloylmethane). Int J Cancer 119:1268–1275
28. Ito S, Ansari P, Sakatsume M, Dickensheets H, Vazquez N, Donnelly RP, Larner AC, Finbloom DS (1999) Interleukin-10 inhibits expression of both interferon a– and interferon gamma–induced genes by suppressing tyrosine phosphorylation of STAT1. Blood 93:1456–1463
29. Hagemann T, Lawrence T, McNeish I, Charles KA, Kulbe H, Thompson RG, Robinson SC, Balkwill FR (2008) "Re-educating" tumor-associated macrophages by targeting NF-kB. J Exp Med 205:1261–1268
30. Hagemann T, Biswas SK, Lawrence T, Sica A, Lewis CE (2009) Regulation of macrophage function in tumors: the multifaceted role of NF-kappaB. Blood 113:3139–3146. https://doi.org/10.1182/blood-2008-12-172825

31. Ohmori Y, Hamilton TA (2001) Requirement for STAT1 in LPS-induced geneexpression in macrophages. J Leukoc Biol 69:598–604
32. Vakkila J, Demarco RA, Lotze MT (2008) Coordinate NF-kB and STAT1 activation promotes development of myeloid type 1 dendritic cells. Scand J Immunol 67:260–269
33. Marotta LLC, Almendro V, Marusyk A et al (2011) The JAK2/STAT3 signaling pathway is required for growth of CD44+ CD24– stem cell–like breast cancer cells in human tumors. J Clin Investig 121:2723–2735. https://doi.org/10.1172/JCI44745
34. Schroder K, Hertzog PJ, Ravasi T, Hume DA (2004) Interferon-gamma: an overview of signals, mechanisms and functions. J Leukoc Biol 75:163–189. https://doi.org/10.1189/jlb.0603252
35. Bontkes HJ, Kramer D, Ruizendaal JJ, Meijer CJ, Hooijberg E (2008) Tumor associated antigen and interleukin-12 mRNA transfected dendritic cells enhance effector function of natural killer cells and antigen specific T-cells. Clin Immunol 127:375–384
36. Hamza T, Barnett JB, Li B (2010) Interleukin 12 a key immunoregulatory cytokine in infection applications. Int J Mol Sci 11:789–806. https://doi.org/10.3390/ijms11030789
37. Kuge S, Watanabe K, Makino K, Tokuda Y, Mitomi T, Kawamura N, Habu S, Nishimura T (1995) Interleukin-12 augments the generation of autologous tumor-reactive CD8+ cytotoxic T lymphocytes from tumor-infiltrating lymphocytes. Jpn J Cancer Res 86:135–139
38. Michel T, Hentges F, Zimmer J (2012) Consequences of the crosstalk between monocytes/macrophages and natural killer cells. Front Immunol 3:403. https://doi.org/10.3389/fimmu.2012.00403
39. Morrison BE, Park SJ, Mooney JM, Mehrad B (2003) Chemokine-mediated recruitment of NK cells is a critical host defense mechanism in invasive aspergillosis. J Clin Invest 112:1862–1870. https://doi.org/10.1172/jci18125
40. Gertsch J, Guttinger M, Heilmann J, Sticher O (2003) Curcumin differentially modulates mRNA profiles in Jurkat T and human peripheral blood mononuclear cells. Bioorg Med Chem 11:1057–1063
41. Kang TH, Lee JH, Song CK et al (2007) Epigallocatechin-3-gallate enhances CD8+ T cell-mediated antitumor immunity induced by DNA vaccination. Cancer Res 67:802–811. https://doi.org/10.1158/0008-5472.CAN-06-2638
42. Bellora F, Castriconi R, Dondero A, Reggiardo G, Moretta L, Mantovani A, Moretta A, Bottino C (2010) The interaction of human natural killer cells with either unpolarized or polarized macrophages results in different functional outcomes. Proc Natl Acad Sci USA 107:21659–21664
43. Verma R, Foster RE, Horgan K, Mounsey K, Nixon H, Smalle N, Hughes TA, Carter CR (2016) Lymphocyte depletion and repopulation after chemotherapy for primary breast cancer. Breast Cancer Res 18:10. https://doi.org/10.1186/s13058-015-0669-x